Early Bone Healing Around 2 Different Experimental, HA Grit-Blasted, and Dual Acid-Etched Titanium Implant Surfaces. A Pilot Study in Rabbits

Luca Gobbato, DDS,* Emilio Arguello, DDS, MS,† Ignacio Sanz Martin, DDS,† Charles E. Hawley, DDS, PhD,‡ and Terrence J. Griffin, DMD, DDS§

Purpose: *To compare early bone healing around different experimental titanium implant surfaces and to evaluate the role of a calcium phosphate–coated implant surface because it relates to bone-implant contact (BIC).*

Methods: *An experimental hydroxyapatite (HA) grit-blasted and dual acid-etched titanium surface (BAE-1) was compared to an experimental HA grit-blasted and dual acid-etched surface treated with nanometer-scale crystals of HA (BAE-2). Both experimental implant surfaces were implanted onto the tibias of 4 New Zealand white rabbits. The animals were killed at 1,6, 21, and 90 days after the implant surgery. Descriptive histology was performed at the healing responses of both implant surfaces. Quantitative morphology assessment provided measurements of BIC, number of bone multicellular units (BMUs), average penetration of BMUs, and maximum penetration of BMUs that were manually made using imaging computer software.*

Result: *The overall BIC for the BAE-2 implant was higher than that for the BAE-1 implant at 21 days of healing. However, there was no significant difference at 90 days of healing.*

Conclusion: *It is concluded from this animal pilot study that the bioactive BAE-2 implant surface provided a better BIC with healthy bone remodeling at 21 days of healing, (Implant Dent 2012;21:454–460)*

Key Words: dental implants, implant surface, calcium phosphate, rabbit, osseointegration

One of the critical factors in bone remodeling and osteogenesis is the early bone healing at the bone-implant interface as Davies[1] described in 2003. Based on this work, a thorough characterization of the effects and processes occurring in bone healing around implants is required to influence bone healing early in the process. The results of this research focused on the cellular responses at early time points after the placement of an implant where they characterized the processes that initiate osseointegration. In the report, the biological cascade of early periimplant bone healing was further explained concluding that by the time the bone is formed on the implant surface, most of the important healing events have already occurred.[1] Other investigators[1,2] have concluded that the osseointegration process observed after implant placement can be compared to bone fracture healing, which is modulated through endocrinal, autocrinal, and paracrinal mechanisms; however, in implant dentistry, the implant surface also possesses excellent biocompatibility because of spontaneous formation of a dense 4-nm layer of titanium dioxide (TiO_2) when it is exposed to air.[2–6] This layer increases calcium deposition and the consequent primary adsorption of adhesive proteins (eg, glycosaminoglycans or albumin), one of the most important events of the initial phase of osseointegration.[2–4]

A recent investigation demonstrated that an acid-etched titanium surface stimulated the expression of markers of osteoblastic phenotype more than a machined titanium surface, as the roughened surface exerts direct effect on mesenchymal stem cells by activating RunX2, a biomarker for osteogenesis and cell differentiation.[7] The implant topography also plays a role in bone healing, as shown by Bagambisa et al[8] who

*Clinical Instructor, Department of Oral Medicine, Infection and Immunity, School of Dental Medicine, Harvard University, Boston MA.
†Clinical Assistant Professor, Department of Oral Medicine, Infection & Immunity, Harvard School of Dental Medicine, Boston MA.
‡Clinical Professor, Department of Periodontology, Tufts University School of Dental Medicine, Boston, MA.
§Associate Professor, Department of Periodontology, Tufts University School of Dental Medicine, Boston, MA.

Reprint requests and correspondence to: Luca Gobbato, DDS MS, Via 20 Settembre 17, Padova 35122, Italy, Phone: 1-617-636-6531, Fax: 1-617-636-0911, E-mail: luca_gobbato@hsdm.harvard.edu

ISSN 1056-6163/12/02106-454
Implant Dentistry
Volume 21 • Number 6

DOI: 10.1097/ID.0b013e3182611cd7

concluded that implant topography may enhance cell attachment, cell adhesion, cell spreading, and cell differentiation.

In addition, other investigators hypothesized that healing of rough surface implants can be improved by the use of bioactive additives such as nanocrystals of calcium phosphate (CaP),[9] which in the presence of a bioactive implant surface enhance the ability to adsorb proteins such as serum proteins, osteopontin and laminin, and cell surface protein and in a similar manner, fibronectin increases the osteoconductivity capacity of the implant itself. However, it is not clear whether it is the microtexture of a microtopographically complex implant surface that plays a key role in enhancing the osteoconductivity of the implant itself, or if the nanocrystals of calcium phosphate (CaP) are the main reason for the increased osteoconductive capacity.[9]

In the same context, it has been demonstrated that the nanocrystals of CaP have the inner ability to readily adsorb proteins on their surfaces.[1,9] The potentiating protein adsorption on the calcium phosphate surface may increase the binding of fibrinogen[9] and other serum proteins that would lead to increased platelet adhesion and thus result in an increased platelet activation accelerating healing.[8,9]

On this matter, and based on the *in vivo* and *in vitro* studies performed by Davies and coworkers,[1,9] it has been suggested that calcium phosphate coating of an implant surface could have a biphasic effect on both platelet activation and fibrin binding.

Aim

The purposes of this pilot study were (a) to evaluate 2 different experimental surfaces, which have no statistically significant differences in their microtexture parameters, and (b) to determine whether the additional surface treatment with nanometer-scale crystals of hydroxyapatite (HA) deposited in a discrete manner (discrete crystalline depositions; Biomet 3i Implant Innovations, Inc, Palm Beach Gardens, FL) plays a role in the early phase of periimplant bone healing.

Many groups have studied the process of osseointegration, but research has mainly focused on the quantification of the bone-to-implant contact (BIC), often comparing the effects of different surface coatings and topographies.[10–15] However, these reports do not provide information on the origin of the bone-implant bond because the quantification is only performed after several months or years of implant healing, therefore omitting early time points. It should be noted that a better understanding of the bone healing events that occur around the implants at the early time points is necessary, "since clinical experience has shown that implant failure often occurs at these early time points."[15–18]

MATERIALS AND METHODS

This study was conducted at the Tufts University School of Dental Medicine and was performed in accordance with the US Food and Drug Administration Good Laboratory Practice regulations set forth in Title 21 Code of Federal Regulations Part 58. This study was approved by the Institutional Animal Care and Use Committee.

Implant Surfaces

The titanium implants used were fabricated especially for this study with 2 different surfaces, varying in composition but not in roughness (3i/Implant Innovations, Palm Beach Gardens, FL). The implants were cylindrical in shape and press fit.

The implant surface morphology was characterized by scanning electron microscopy (SEM) (JSM-6460LV; JEOL) and field emission SEM (JSM-6700F; JEOL, Musashino Chome Akishima, Tokyo, Japan). A noncontact interferometer (MicroXAM; KLA Tencor/ADE Phase Shift, Milpitas, CA) was used to characterize the surface topography and amplitude (Sq, Sa) (Fig. 1, A–C).

The titanium surface used as a control group (BAE-1), was an HA grit-blasted and dual acid-etched cylindrical type titanium implant (blasted and acid-etched, BAE) with an absolute mean height (peak-trough) deviation (Sa) equal to 0.902 μm. The titanium surface used as a test group had an additional surface treatment where nanometer-scale crystals of HA were deposited in a discrete manner (discrete crystalline depositions) covering approximately 50% of the osseous-contacting surface with an absolute mean height (peak-trough) deviation (Sa) equal to 0.897 μm.

SURGICAL PROCEDURES

Four New Zealand white rabbits were selected to be part of the study. The left and the right tibial epiphyses were randomly selected to receive 2 BAE-1 mini-implants and 2 BAE-2 mini-implants, respectively (Fig. 2). A total of 16 implants were placed in sterile conditions, the animal were preanesthetized by an intramuscular injection of 5.6 mg/kg of xylazine and 0.19 mg/kg of acepromazine. The anesthesia was given by intravenous injection of 4.0 mg/kg of ketamine and 1.0 mg/kg of xylazine. Administration of analgesic agents (0.05 up to 0.1 mg/kg of buprenorphine) was provided to all animals, half dose at the induction of anesthesia and the other half at the end of the surgery.

A 10-mm skin incision was made to provide access to the bone. Implantation sites were prepared by drilling an osteotomy, while profuse irrigation with sterilized physiologic saline was maintained. After the implantation, the skin was sutured, leaving the implants submerged.

The animals were killed after 1, 6, 21, and 90 days after implantations. At the end of the experiment, the animals were killed under general anesthesia, by an injection of sodium pentobarbital with an 86 mg/kg of sodium pentobarbital and 11 mg/kg of phenytoin.

Histologic Preparation

Immediately after killing animals, epiphyseal specimens were collected. The samples of the animals were fixed in 2% paraformaldehyde.

Bone segments with implants were fixed by immersion in $CaCO_3$-buffered formalin solution, dehydrated, and embedded in poly-methyl methacrylate. Because implants remained in these samples, ground sections of approximately 100 μm were made parallel to the implant axis, using a diamond saw. These sections were stained with Stevenel blue and Goldner stain to differentiate among bone, osteoid, and connective tissue.

Descriptive Histology

Histological slides were illuminated with a combination of transmitted

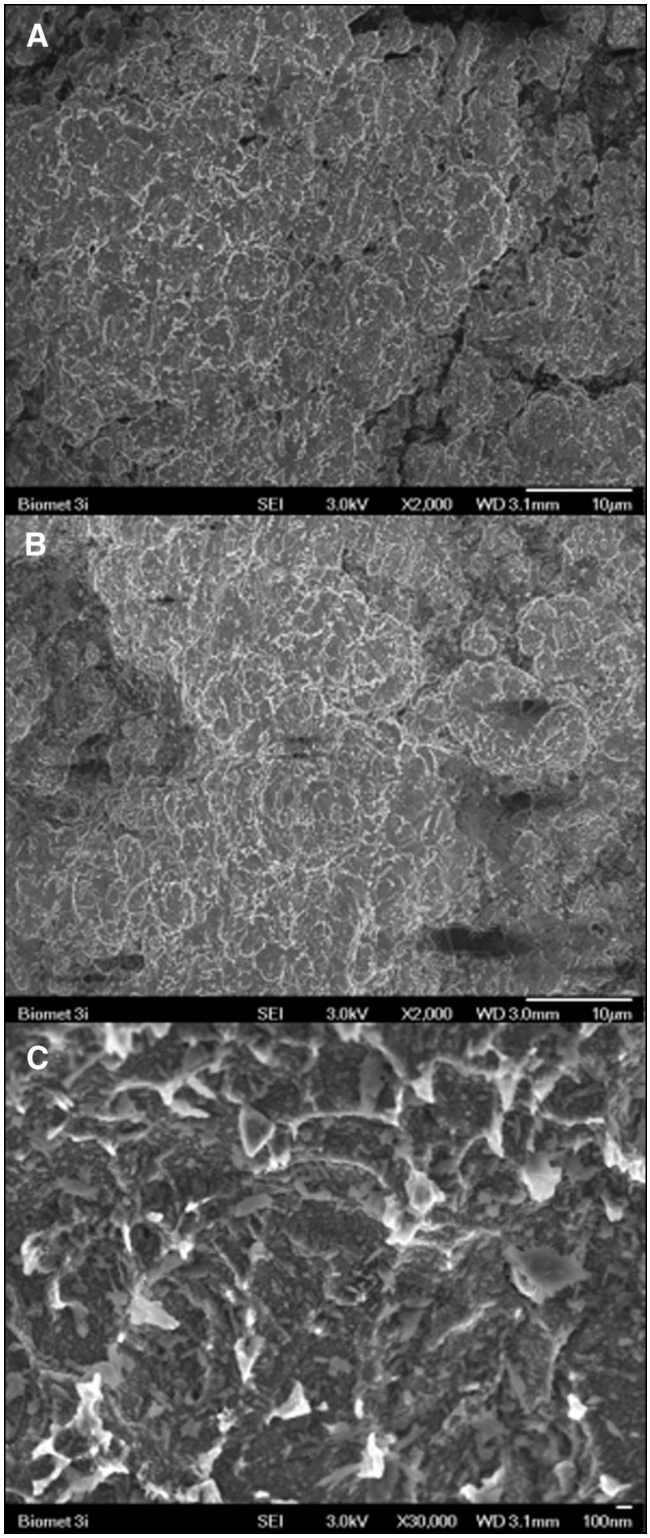

Fig. 1. A and **B,** The implant surface morphology was characterized by SEM (JSM-6460LV; JEOL) and field emission SEM (JSM-6700F; JEOL). A noncontact interferometer (MicroXAM; KLA Tencor/ADE Phase Shift) was used to characterize surface topography and amplitude (Sq, Sa). **C,** With higher magnification, it is possible to appreciate the deposition of the CaP at the implant surface. Crystals of HA are deposited in a discrete manner (discrete crystalline depositions) covering approximately 50% of the osseous-contacting surface with an absolute mean height (peak-trough) deviation (Sa) equal to 0.897 μm.

and reflected white light using an Olympus BX40 microscope. Digital images were collected at magnifications of ×10, ×20, ×40, or ×80, depending on the feature of interest, using Qimaging Micropublisher 3.3 digital camera with Image Pro Plus software (Version 7.0; MediaCybernetics, Bethesda, MD). To obtain a composite image of the entire implant surface, a series of high-resolution images (2048 × 1536 pixels/field) were taken along the implant from periosteal to endosteal cortical surface including the entire implant interface within the marrow cavity. Image fields were tiled into a single high-resolution image encompassing the entire region of interest.

Quantitative morphology assessment provided measurements of BIC, number of bone multicellular units (BMUs), average penetration of BMUs, and maximum penetration of BMUs that were manually made using Image computer software.

The histomorphometric parameters (Table 1) measured were the area of new bone (new bone), the BIC (overall BIC) relative to the total implant perimeter, the BMUs, average penetration, and the maximum penetration within native cortical bone adjacent to the implant surface.

The blood clot area, fibrin network with entrapped erythrocytes, was measured in 1 section per implant, and the average blood clot area was calculated.

The new bone within a 400-μm distance from the implant was measured by color differentiation of the Stevenel blue–stained specimens. Only new bone was measured, and the native cortical bone interface was not included in the area measurement.

To calculate BIC, the surface area of the implant within the cortical width was measured and the total surface area of the implant measured from the periosteal contact point at one edge of the implant to the periosteal contact point at the opposite edge of the implant. The BIC of the overall implant was calculated by dividing the overall bone contact length by the entire perimeter of the implant (Fig. 2).

BMU measurements were made on the Goldner-stained samples. BMUs are defined as organized structures of

groups of osteoclasts and osteoblasts together with blood vessels, and when present in cortical bone, they are often called cutting cones (Fig. 3). The total number of BMUs was counted. The distance of the leading edge (edge furthest from implant surface) of each BMU was measured, and the average and maximum BMU penetration was calculated for each slide.

RESULTS

There were no unscheduled deaths among the animals. In all animals, the healing was uneventful, and infection was not observed after any implant placement.

Histology

One day after implant placement, a network of fibrin containing a large number of erythrocytes was observed at the implant interface. No differences were noted between the sizes of blood clot between implant surfaces at any time point. The BAE-2 implant surface induced mesenchymal stem cell (MSC) migration to the implant surface within a day of implantation, whereas the BAE-1 implant surface was slower to induce cell attachment. The MSC proliferation and migration increased with time for both implant surfaces (Fig. 4, A and B).

After 6 days, red blood cells at the implant cavity were replaced by osteoclasts and osteoblasts. Both the BAE-1 and BAE-2 implant surfaces produced similar osteoid responses at the cortical bone-implant interface. A transient increase in osteoid at the bone-implant interface was noted at 6 days with little or no interfacial unmineralized matrix was seen at all other time points.

The osteocytic bone score was based on extent of necrotic or osteocytic cortical bone adjacent to the implant. The data showed that a minimal amount of necrotic osteocytes were noted at 6 days adjacent to the implant surface.

The cellular remodeling of the bone fragments was similar between the treatment groups and activity peaked at 6 days after implantation. BMUs appeared in the preexisting bone, which initiated bone remodeling. Similar amounts of bone were formed within a 400-μm perimeter of the implant surface in both

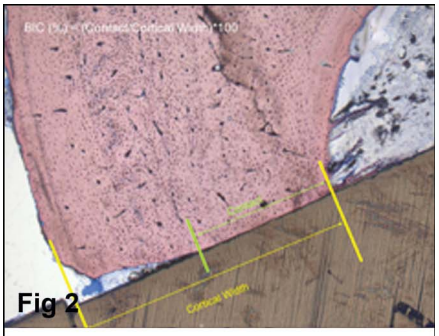

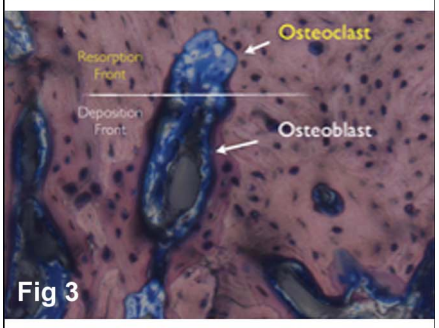

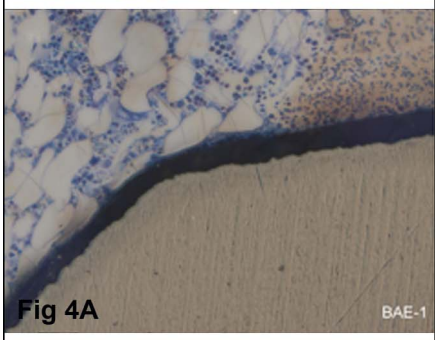

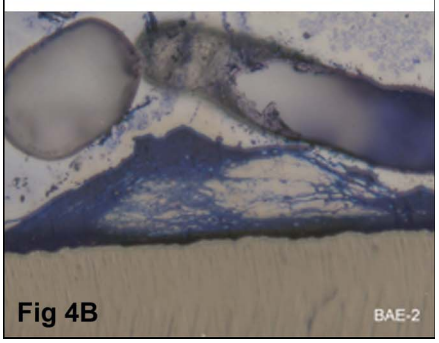

Fig. 2. BIC within the cortical width at the site of implantation was calculated by dividing the bone contact length by the perimeter of the implant along the entire cortical width. This image is from a BAE-2 implant placed in the distal position in the tibia after 6 days of healing (Stevenel blue stain, magnification of original image, ×40).

Fig. 3. Cutting Cones for BAE-2 (higher magnification) illustrating a so-called BMU, which is present in bone tissue undergoing active remodeling. The presence of a resorption front with osteoclast and a deposition front that contains osteoblasts and osteoid were noted. Vascular structures occupy the central area of the BMU.

Fig. 4. A and **B,** MSCs on BAE-2 implant surfaces at day 1. Erythrocytes are the dominant cell type adjacent to the BAE-1 implant, whereas MSC and fibroblast-like cells have started to create a network on the BAE-2 implant. Images were acquired of specimens with the Stevenel blue stain at a magnification of ×80.

Table 1. Quantitative Morphology Analysis

Quantitative Parameter	Description	Units of Measurement
New bone	Area of new bone formed within 400 μm of the implant surface. This measurement does not include native bone within the cortical width	Square millimeter
Overall BIC	BIC relative to the total implant perimeter. The implant perimeter was measured from the points at which the implant interfaced with the periosteal bone surface. Similarly, the BIC was measured along the entire implant. The percent overall BIC was calculated by dividing the total BIC by the total implant perimeter	Percent
BMUs	Number of bone remodeling units within native cortical bone	Count
Ave BMU	Average penetration of remodeling cutting cones into the native cortical bone adjacent to the implant surface	Micrometer
Max BMU	Maximum penetration of remodeling cutting cones into the native cortical bone adjacent to the implant surface	Micrometer

New bone indicates the area of new bone; overall BIC, the BIC relative to the total implant perimeter; ave BMU, average penetration; max BMU, maximum penetration.

surfaces at both 6 and 21 days after implantation (Fig. 5). Both treatment groups showed a steady increase in the overall BIC up to 21 days, with a greater increase noted for the BAE-2 compared to the BAE-1 treatment between 6 and 21 days (Fig. 6, A and B).

The BAE-2 implant had notably greater maximum BMU penetration into the adjacent cortical bone compared to the BAE-1 implant between 6 and 21 days of healing (Fig. 6, C and D). The maximum BMU penetration increased between 6, 21, and 90 days for both the treatment groups. After 90 days of healing, the average BMU penetration was similar for both implants, as the overall BIC.

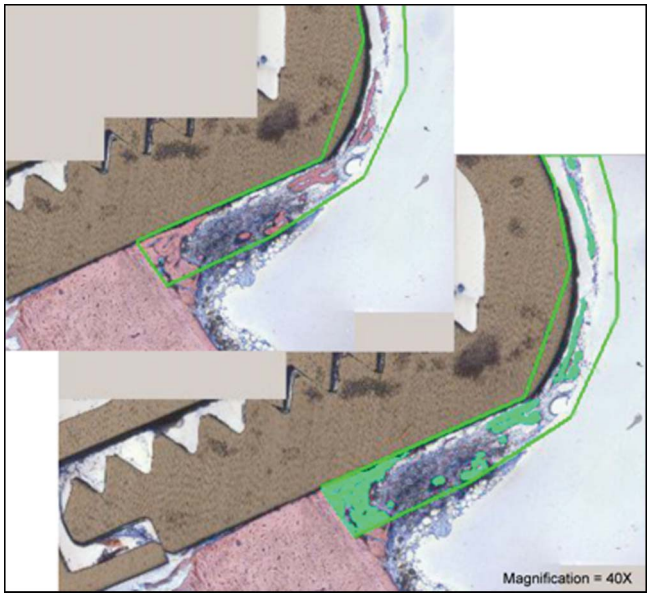

Fig. 5. Area of new bone measured within 400 μm of the implant surface. The top image is the region of interest providing the boundaries for bone measurement. The bottom image shows the bone thresholded to "green," and the area of the thresholded bone was measured. The original native cortical bone was not included in the "new bone" area measurement. The image in this example is from a nanotite implant placed in the distal position in the tibia after 21 days of healing (Stevenel blue stain, magnification of original image: ×40).

Histomorphometry

To understand the healing mechanisms of bone surrounding implants, quantitative morphology assessment provided measurements of BIC, number of BMUs, average penetration of BMUs, and maximum penetration of BMUs that were manually made using an imaging computer software.

Measurement of BIC on Ground Poly-methyl Methacrylate Sections

Both the treatment groups showed a steady increase in the overall BIC up to 21 days, with a greater increase noted for the BAE-2 compared to the BAE-1 treatment between 6 and 21 days. The overall BIC for the BAE-2 implant was 53.1% higher than that for the BAE-1 implant at 21 days and 20% higher at 90 days of healing.

Measurement of BMU

Approximately twice the number of BMUs was present in the cortical bone surrounding the implant for the BAE-2 implant compared to the BAE-1 implant at both 6 and 21 days. After 90 days of healing, 34% more BMU were counted for the BAE-2 implant compared to the BAE-1 implant. The number of BMUs increased to almost double between 6 and 21 days for both the treatment groups and leveled out by 90 days. At 6 days, the BMU penetration was 58% greater for the BAE-2 compared to the BAE-1 implant. At 21 days, the BAE-2 implant had an average BMU penetration 44.5% greater than the BAE-1 implant. After 90 days of healing, the average BMU penetration was similar for both implants with the BAE-1 implant having slightly greater penetration compared to the BAE-2 implant.

The average BMU penetration increased slightly between 6 and 21 days for both the treatment groups. The BMU penetration increased more than double between 21 and 90 days. Similar to the average BMU penetration, the maximum penetration of BMUs into the adjacent cortical bone was notably greater for the BAE-2 implant compared to the BAE-1 implant at both 6 and 21 days and had similar maximum penetration at 90 days.

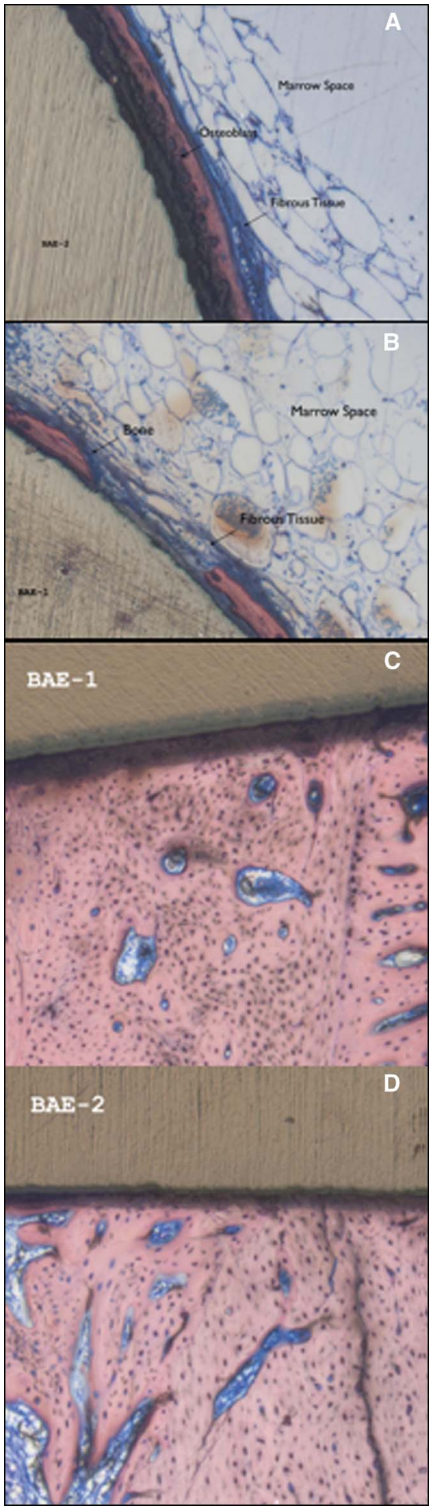

Fig. 6. **A** and **B,** BAE-1 and BAE-2 (left and right side, respectively) showing BIC after 21 days of healing. The BIC after 21 days was 53.1% more on the BAE-2 when compared to the BAE-1 group. In the picture, we can appreciate a thin layer of osteoblast depositing new bone over the implant surface. This phenomenon is better described over the BAE-2 surface. **C** and **D,** The BAE-2 implant had notably greater maximum BMU penetration into the adjacent cortical bone compared to the BAE-1 implant at 21 days of healing. BMU count was performed around the total perimeter of each implants. Penetration of BMU (average penetration and maximum penetration) was scored as well.

DISCUSSION

Although many variables exist when examining the healing response around titanium or titanium-alloy implants, one could argue that the addition of certain biocompatible materials such as calcium phosphate could enhance the BIC. When looking at the preliminary studies on bioactive glasses carried out by Hench and Wilson,[19] 2 classes of endosseous implants were identified: bone bonding and nonbonding. In this matter, in the past 2 decades, we have seen increasing attempts to change the passive interfacial coexistence associated with bioinert implants to arrive to the so-called bioactive or bioreactive design, which utilizes materials for the purpose of enhancing interactions between the implant and the host tissue as if the fixture was equivalent to the host tissue itself.[20] In addition, it should be pointed out that metals such as titanium are nonbone bonding, whereas calcium phosphate materials are considered bone bonding. However, the concept of a bone-bonding material is quite irrelevant if we think, as Davies has described, that by the time that bone is formed around the implant, the major events that regulate the phenomena of bone formation have already occurred. On the other hand, the reported role of protein absorption as described in the literature is probably one of the most important events that regulate the osteogenic capacity of the implant surface.[20]

In a rabbit model, Sul et al[21] compared 3 different implant surfaces: oxidized magnesium (Mg), TiUnite, and Osseotite. Surface roughness evaluations revealed similar Sa values for Mg and Osseotite implant, which were minimally rough (Sa, 0.69 and 0.72 μm, respectively) compared to the moderately rough TiUnite implants (Sa, 1.35 μm). Based on these values, it is clear that TiUnite implants were strongly favored with respect to their moderately roughened surface, and yet they did not achieve the greatest bone integration. As the results showed the Mg implant achieved a significant BIC value due to its chemical/physical surface characteristics rather than topographic or design characteristics. Overall, these results support the hypothesis that bioactive

surface chemistry favors fast and strong integration of implants in bone at healing periods earlier than 6 weeks.

Moreover, in our study, the BMU value was scored for both experimental implant surfaces. BMU penetration was significantly higher in the BAE-2 group, showing BMU penetration 58% greater for the BAE-2 compared to the BAE-1 implant at 6 days. At 21 days, the BAE-2 implant had an average BMU penetration 44.5% greater than the BAE-1 implant; additionally, newly formed bone was first detected after 6 days of healing. This time frame of new bone formation is in agreement with the study by Piattelli et al[22] showing osteoid deposition 1 week after the placement of screw-shaped implants in the articular femoral knee joint of the rabbit. There were differences observed between healing of trabecular bone versus cortical bone. The remodeling of trabecular bone by the BMUs started after 6 days of healing, whereas the cortical bone needed a time span of 3 weeks to initiate the remodeling of the preexisting bone surrounding the implant. A faster process was also seen when comparing the new bone formation around the implant. In trabecular bone, osteoid was observed after 6 days of healing, whereas in cortical bone, new bone was first detected only after 3 weeks of healing. The BIC after 90 days was higher in cortical bone, which is in accordance with the findings by Sennerby et al[23] who used screw-shaped titanium implants in the rabbit tibia and femoral part of the knee joint. However, our study showed that the increase in BIC initiated earlier in the trabecular bone when compared to the cortical bone.

CONCLUSIONS

In this rabbit study, the presence of MSC on the BAE-2 surface at early time points promoted a faster healing process of the new bone around the implant surface when compared to the BAE-1 surface. The chemical modification of a moderately rough implant surface improved the process involved in osseointegration.

Further research such as clinical trials of early loading over the presented experimental implant surfaces should be initiated to better demonstrate the significance of these findings.

DISCLOSURE

The authors claim to have no financial interest in any companies or products mentioned in this article. None of the participants in the groups reported a conflict of interest.

ACKNOWLEDGMENT

This study was supported by Biomet 3i, Palm Beach Gardens, FL. The authors mention their gratitude to Dr J. Kenealy, Clinical Research Department, Implant Innovations, Inc, Palm Beach Gardens, FL.

REFERENCES

1. Davies JE. Understanding peri-implant endosseous healing. *J Dent Educ*. 2003;67:932–949.

2. Romanos G, Toh CG, Siar CH, et al. Peri-implant bone reactions to immediately loaded implants. An experimental study in monkeys. *J Periodontol*. 2001;72:506–511.

3. Avila G, Misch K, Galindo-Moreno P, et al. Implant surface treatment using biomimetic agents [review]. *Implant Dent*. 2009;18:17–26.

4. Rezania A, Healy KE. Integrin subunits responsible for adhesion of human osteoblast-like cells to biomimetic peptide surfaces. *J Orthop Res*. 1999;17:615–623.

5. Liu Y, de Groot K, Hunziker EB. Osteoinductive implants: the mise-en-scene for drug-bearing biomimetic coatings. *Ann Biomed Eng*. 2004;32:398–406.

6. Abrahamsson I, Berglundh T, Linder E, et al. Early bone formation adjacent to rough and turned endosseous implant surfaces. An experimental study in the dog. *Clin Oral Implants Res*. 2004;15:381–392.

7. Marinucci L, Balloni S, Becchetti E, et al. Effect of titanium surface roughness on human osteoblast proliferation and gene expression in vitro. *Int J Oral Maxillofac Implants*. 2006;21:719–725.

8. Bagambisa FB, Joos U, Schilli W. Interaction of osteogenic cells with hydroxylapatite implant materials in vitro and in vivo. *Int J Oral Maxillofac Implants*. 1990;5:217–226.

9. Mendes VC, Moineddin R, Davies JE. Discrete calcium phosphate nanocrystalline deposition enhances osteoconduction on titanium-based implant surfaces. *J Biomed Mater Res A*. 2009;90:577–585.

10. Choi JY, Lee HJ, Jang JU, et al. Comparison between bioactive fluoride modified and bioinert anodically oxidized implant surfaces in early bone response using rabbit tibia model. *Implant Dent*. 2012;21:124–128.

11. Jimbo R, Fernandez-Rodriguez J, Sul YT, et al. Principal component analysis: a novel analysis to evaluate the characteristics of osseointegration of different implant surfaces. *Implant Dent*. 2011;20:364–368.

12. Veis AA, Dabarakis NN, Parisis NA, et al. Bone regeneration around implants using spherical and granular forms of bioactive glass particles. *Implant Dent*. 2006;15:386–394.

13. Brånemark PI, Adell R, Albrektsson T, et al. Osseointegrated titanium fixtures in the treatment of edentulousness. *Biomaterials*. 1983;4:25–28.

14. Albrektsson T, Wennerberg A. Oral implant surfaces: part 1—review focusing on topographic and chemical properties of different surfaces and in vivo responses to them. *Int J Prosthodont*. 2004;17:536–543.

15. Albrektsson T, Wennerberg A. Oral implant surfaces: part 2—review focusing on clinical knowledge of different surfaces. *Int J Prosthodont*. 2004;17:544–564.

16. Jaffin RA, Berman CL. The excessive loss of Branemark fixtures in type IV bone: A 5-year analysis. *J Periodontol*. 1991;62:2–4.

17. Raghavendra S, Wood MC, Taylor TD. Early wound healing around endosseous implants: a review of the literature. *Int J Oral Maxillofac Implants*. 2005;20:425–431.

18. Trisi P, Todisco M, Consolo U, et al. High versus low implant insertion torque: a histologic, histomorphometric, and biomechanical study in the sheep mandible. *Int J Oral Maxillofac Implants*. 2011;26:837–849.

19. Hench LL, Wilson J. Surface-active biomaterials. *Science*. 1984;226:630–636.

20. Schwartz Z, Boyan BD. Underlying mechanisms at the bone-biomaterial interface. *J Cell Biochem*. 1994;56:340–347.

21. Sul YT, Johansson C, Albrektsson T. Which surface properties enhance bone response to implants? Comparison of oxidized magnesium, TiUnite, and Osseotite implant surfaces. *Int J Prosthodont*. 2006;19:319–328.

22. Piattelli M, Scarano A, Paolantonio M, et al. Bone response to machined and resorbable blast material titanium implants: an experimental study in rabbits. *J Oral Implantol*. 2002;28:2–8.

23. Sennerby L, Thomsen P, Ericson LE. A morphometric and biomechanic comparison of titanium implants inserted in rabbit cortical and cancellous bone. *J Oral Maxillofac Implants*. 1992;7:62–71.